

Temporal declines in Wadden Sea phytoplankton cell volumes observed within and across species

Helmut Hillebrand ^{1,2,3*} Josie Antonucci Di Carvalho ^{2,3} Jan-Claas Dajka ^{1,2} Claus-Dieter Dürselen,⁴
Onur Kerimoglu ⁵ Lucie Kuczynski ¹ Lena Rönn,⁶ Alexey Ryabov ⁵

¹Institute for Chemistry and Biology of Marine Environments (ICBM), Carl-von-Ossietzky University Oldenburg, Wilhelmshaven, Germany

²Helmholtz Institute for Functional Marine Biodiversity at the University of Oldenburg (HIFMB), Oldenburg, Germany

³Alfred Wegener Institute, Helmholtz Centre for Polar and Marine Research (AWI), Bremerhaven, Germany

⁴AquaEcology GmbH & Co. KG, Oldenburg, Germany

⁵Institute for Chemistry and Biology of Marine Environments (ICBM), Carl-von-Ossietzky University Oldenburg, Oldenburg, Germany

⁶Lower Saxony Water Management, Coastal Defence and Nature Conservation Agency (NLWKN, Brake-Oldenburg), Oldenburg, Germany

Abstract

Cell size is a master trait in the functional ecology of phytoplankton correlating with numerous morphological, physiological, and life-cycle characteristics of species that constrain their nutrient use, growth, and edibility. In contrast to well-known spatial patterns in cell size at macroecological scales or temporal changes in experimental contexts, few data sets allow testing temporal changes in cell sizes within ecosystems. To analyze the temporal changes of intraspecific and community-wide cell size, we use the phytoplankton data derived from the Lower Saxony Wadden Sea monitoring program, which comprises sample- and species-specific measurements of cell volume from 1710 samples collected over 14 yr. We find significant reductions in both the cell volume of most species and the weighted mean cell size of communities. Mainly diatoms showed this decline, whereas the size of dinoflagellates seemed to be less responsive. The magnitude of the trend indicates that cell volumes are about 30% smaller now than a decade ago. This interannual trend is overlaid by seasonal cycles with smaller cells typically observed in summer. In the subset of samples including environmental conditions, small community cell size was strongly related to high temperatures and low total phosphorus concentration. We conclude that cell size captures ongoing changes in phytoplankton communities beyond the changes in species composition. In addition, based on the changes in species biovolumes revealed by our analysis, we warn that using standard cell size values in phytoplankton assessment will not only miss temporal changes in size, but also lead to systematic errors in biomass estimates over time.

Introduction

Trait-based approaches to community ecology have been advanced to promote a mechanistic link between species' characteristics and their functional performance (Violle et al. 2007). Functional classifications have a long history when analyzing plant composition (Raunkiaer 1907), which led to systematically building representative trait databases

(Kleyer et al. 2008; Kattge et al. 2011; Weigelt et al. 2020). Instead of grouping species into functional group categories, such databases comprise continuous axes of measurable characteristics, which enable global analyses of how traits affect plant distribution and performance and thus spatial and temporal dynamics in communities (Craine et al. 2005; Suding et al. 2008; Bruelheide et al. 2018).

Although phytoplankton is responsible for roughly the same fraction of the global net primary production as terrestrial plants, trait-based approaches to their ecology have been introduced at a much later stage (Litchman and Klausmeier 2008). While functional classifications of phytoplankton have been used for decades (Margalef 1978; Reynolds 1984; Verity and Smetacek 1996), comparable global trait databases are missing. However, recent years have seen a quickly growing body of

*Correspondence: helmut.hillebrand@uni-oldenburg.de

This is an open access article under the terms of the Creative Commons Attribution-NonCommercial-NoDerivs License, which permits use and distribution in any medium, provided the original work is properly cited, the use is non-commercial and no modifications or adaptations are made.

Additional Supporting Information may be found in the online version of this article.

literature systematically assessing phytoplankton traits to explain processes from ecophysiological to global ecosystem scales (Litchman et al. 2007; Follows and Dutkiewicz 2011; Mutshinda et al. 2017).

In these endeavors, cell size has quickly been identified as a highly reliable master trait that summarizes a range of constraints in resource uptake, storage and growth in overarching allometric scaling laws (Litchman et al. 2007; Marañón 2015; Hillebrand et al. 2021). The range of cell sizes in phytoplankton encompasses nine orders of magnitude (Finkel et al. 2010), which exceeds the size range of mammals or plants. Larger cells have higher maximum cell-specific nutrient uptake rates, higher carbon fixation rates and higher cellular nutrient content (Litchman et al. 2007, Hillebrand et al. 2021). Larger cells have higher cell-specific but lower volume-specific affinity to both nitrogen and phosphorus and exhibit lower maximum growth rates (Edwards et al. 2012). Also, light affinity and carbon assimilation depend on cell size (Edwards et al. 2015; Malerba et al. 2021). At the same time, size is decisive in constraining vulnerability to grazing (Kiørboe 1993; Irigoien et al. 2005; Branco et al. 2020), nutrient storage capacity (Grover 1991; Litchman et al. 2009; Kerimoglu et al. 2012), or mobility (Sommer 1988).

Consequently, phytoplankton cell size has become a sentinel of global change, especially at the community level through analyzing community weighted means cell size. Given the tight relationships between size and nutrient affinity (Irwin et al. 2006), eutrophication tends to foster larger celled phytoplankton (Larsson and Hagström 1982). With respect to warming, both experiments (Sommer and Lengfellner 2008; Lewandowska and Sommer 2010; Yvon-Durocher et al. 2011) and observations (Winder et al. 2009; Mousing et al. 2014; Rasconi et al. 2015) find smaller species to dominate at higher temperatures. These findings are backed up by macroecological studies finding smaller cell sizes at high temperatures (Moran et al. 2010; Acevedo-Trejos et al. 2013), which can be found at lower latitudes (Acevedo-Trejos et al. 2018) in combination with low nutrient concentrations (Mousing et al. 2018).

In contrast to our knowledge on these spatial patterns, information on temporal changes in size is rare on ecological time scales (but see DuRand et al. 2001; Wiltshire et al. 2008; Huete-Ortega et al. 2010). Moreover, this temporal information is often at the community level of size spectra (e.g., from flow cytometric analyses) or mean cell size, which do not allow disentangling whether observed changes in time reflect changes in species composition or intraspecific changes in size. The former indicates competitive displacement, when small species replace large species, whereas the latter indicates a physiological or adaptive response at the population level.

Here we use a unique monitoring data set that measures species-specific abundances and cell sizes, the latter by independently measuring multiple individuals per species and sample. Spanning 14 consecutive years (2006–2019) and

weekly to monthly sampling at different stations in the Lower Saxony section of the Wadden Sea, this data set allows testing a set of hierarchical hypotheses. First, we generally test whether cell sizes in the phytoplankton change over time (H1) using all cell size measurements available in the data set. If so, we disentangle between community and population responses: we test whether changes in cell size are significant within species by assessing species-specific slopes of size dependence on time (H2). For communities, we use community-weighted mean cell size for each sample and test for temporal trends at the community level (H3). Finally, we test whether the temporal change in mean cell size can be related to environmental factors, such as nutrients and temperature (H4).

Methods

Sites

Since the end of the 1980s, the Lower Saxony Water Management, Coastal Defense and Nature Conservation Agency (NLWKN) conducts year-round phytoplankton monitoring in Lower Saxony's coastal waters (Hanslik et al. 1998). From 2006 onwards, the monitoring program additionally comprises cell volume measurements at species level, which has been used to calculate total biovolume by multiplying abundances with average cell volume. Our analysis comprises the data from 2006–2019, which derive from 20 stations in the coastal waters of Lower Saxony, Germany (Supporting Information Fig. S1). Whereas some of these stations were continuously monitored, others have been used only for shorter periods of time or at reduced frequency (Supporting Information Fig. S1). In total, 1710 samples were analyzed for this study.

Sampling

Sampling occurred year-round in most cases, but for some stations covered the vegetation period only, extending from beginning of March to the end of September/October (NLWKN 2013). Water samples were obtained as a bucket sample from the surface (max. of 1 m depth) and each sample was mixed from three scooping processes in one 5-liter canister per station and date. Samples were fixed with Lugol's iodine solution and stored in a cool and dark place until microscopical analysis. Storage times of preserved samples were approximately the same in each year as analyses of samples started in the end of one monitoring season. Environmental parameters obtained included temperature, salinity, pH, suspended particulate matter (SPM), and nutrients, which were not recorded at all places and all times, but in four "main" stations (Supporting Information Fig. S1). The analysis of nutrients followed seawater analysis procedures (Grasshoff et al. 1983). Total nutrients were derived from unfiltered samples, digesting total nitrogen (TN) and total phosphorus (TP) by heat and pressure or by microwave with peroxodisulfate

(Koroleff digestion). Dissolved orthophosphate, nitrate and nitrite as well as dissolved silicate (Si) were measured photometrically. Salinity, pH, and temperature were measured using a multisensor (WTW Multisonde 3430). SPM was measured as the dry weight of filtered seston. Supporting Information Fig. S2 presents the temporal changes in most of these variables.

Microscopy

Phytoplankton samples were analyzed for taxonomic composition, species-specific abundance and the estimation of biovolume using an inverted microscope according to Utermöhl (1958). Microscopic analyses allow quantification of cells $> 3 \mu\text{m}$, thus do not cover picoplankton extensively. While to our knowledge there is no systematic assessment of the contribution of picoplankton in the Wadden Sea, others reported a dominance of larger phytoplankton under the rather nutrient-rich conditions in this area (Philippart et al. 2000; Prins et al. 2012). For the taxa observed, identification to species level was preferred, but if not possible, taxa were categorized at lowest detectable taxonomic levels. In total, a minimum of 400 individuals per sample were counted at different microscopic magnifications (up to $\times 400$) corresponding to size, allowing to detect individuals down to a size of around $2\text{--}3 \mu\text{m}$ such as *Phaeocystis* and other small flagellates and coccal algae. The biomass-rich and most abundant taxa were usually recorded with a minimum number of 20–60 cells depending on magnification. For each taxon, size and geometry of a representative number of the cells were determined to estimate the biovolume of each phytoplankton taxa in a sample (taxon-specific and total biovolume). The biovolume of phytoplankton species was determined according to the procedure standardized by the European Committee for Standardization for “Guidance on the estimation of phytoplankton biovolume”, which has been published in all European Union member states as a standard document (in Germany as DIN EN 16695:2015-12, <https://doi.org/10.31030/2303923>). All volumes are on a per-cell basis, that is, for chain-forming species the volumes of single cells in the chains are measured.

Data integration

Prior to analyses, we harmonized the use of the biovolume calculations, switching all geometric models to the above-mentioned standard norm. For each genus, we made sure that the dimensions for the geometric models were used consistently over time. A recurrent problem in biovolume calculation is the third (hidden) dimension, that is, the height of a prism or the small diameter of an ellipsoid, which often is not directly measurable under the microscope. Here, we followed the guidance by the European Committee for Standardization to estimate the missing dimension per species using a constant average ratio to another dimensions. The accuracy of such proposed factors for hidden dimensions has been analyzed for monitoring procedures (Olenina et al. 2006). Thus,

the observed difference in cell size relies on individual measurements of two dimensions per specimen, whereas the third dimension is a function of the first two. We removed all purely heterotrophic species identified and harmonized the taxonomy using the phylogenetic tree used in Algaebase (Guiry and Guiry 2021). We additionally flagged all species that were not identified to species level. We primarily focus our statistical analyses on the subset of species identified to species level, as our hypotheses explicitly comprise intraspecific changes. However, we provide analogous analyses including all taxa (details see “Sensitivity analyses”). We calculated mean cell size for each unique sample (each sampling day and station) as weighted means, for which we created mean ln-transformed cell sizes (i.e., geometric means) for each species, and then calculated the abundance-weighted mean across species. Here, we only used samples with at least 10 cells being measured to avoid mean cell size estimates based on very small sample sizes.

Statistical analyses

For the first three hypotheses, we created generalized linear mixed models (GLMMs) using the lme4 package version 1.1.-26 (Bates et al. 2015) in R (R Development Core Team 2018; RStudio Team 2018). To generally test for temporal changes in cell size (hypothesis H1), our model comprised year and Julian day as continuous fixed effects and stationID, yearID and taxonomy as categorical random effects. A significant temporal trend across years would reject the null hypothesis to H1 (i.e., cell size did not change over time). We added Julian day as second fixed effect to account for seasonal differences in cell sizes. As the raw Julian day comprise lowest and highest values in winter, while summer has intermediate values, we transformed Julian day to increasing until the mid of the year (Julian Day = 183) and then decreasing again. Thereby, this transformed Julian Day variable reflects the transition towards “summeriness.” As size has strong phylogenetic constraints, taxonomy was added as a nested random term with species nested in genus, in order, in class and in phylum, which allows for different intercepts at all these taxonomic organizational levels. Given very uneven distribution of measurements across taxa, we refrained from adding random slopes as well; instead, differences in species-specific slopes are explicitly considered in the analysis of H2. In addition, we allow for different intercepts at different stations (stationID) and in different years (yearID). Adding a random yearID effect in models on temporal dynamics has been highly recommended (Daskalova et al. 2021), because year as a continuous fixed effect tests the hypothesis, whereas yearID as a categorical random effect allows for different intercepts, which could, for example, reflect unusual conditions in certain years (but see alternative approaches under “Sensitivity analyses”). We used the autocorrelation function in R to check for temporal autocorrelation in the model, which however was negligible. Thus, we did not conduct autoregressive models here. We used the

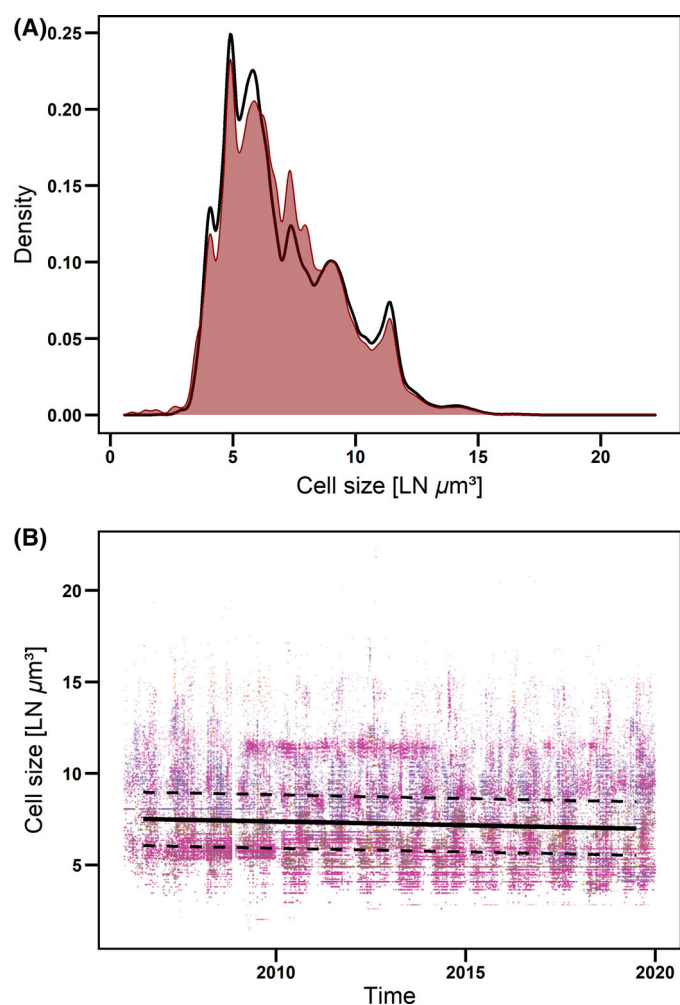


Fig. 1. (A) Density plot of all measured cell sizes across the entire 1710 samples analyzed in the NLWKN monitoring data. Black line is the density for the reduced data set (identified to species level); the red area is the density of the full data set (including algae not identified to species level). (B) Single cell size measurements over time, colors represent classes (the most dominant are listed in Fig. 2). Black line is the significant fixed effect of time (year), dotted lines the 95% CI of the predicted effect.

GLMM with year and transformed Julian Day as fixed effects and year ID, stationID and phylogeny as random effects for all measured cells identified to species level ($N = 273,888$). This approach provides more data points for more abundant and dominant species. Therefore, we reran this model using sample means per species, that is, the average cell size per species per station and date ($N = 29,678$).

To explicitly test for intraspecific changes in size (H2), we conducted separate GLMMs analogous to the above for each species, with year and transformed Julian Day as continuous fixed effects and stationID and yearID as categorical random terms. As the models were species specific, the nested random term on taxonomy used in the main model was not included. To avoid biased estimates from species that occurred only very

rarely or only in a short time window, we only used species occurring over a period of at least 5 yr and represented by at least 100 measured cells. In addition to interpreting the species-specific slopes, we tested whether the slopes generally were different from 0. For this, we conducted a random effect weighted meta-analysis using the “metafor” package in R version 3.0-2 (Viechtbauer 2010). We used the GLMM slope estimate with year as an effect size and its standard error as sampling variance and obtained the overall slope across all species-specific changes in cell size.

The analysis of weighted mean cell size (H3) was conducted in a similar way as for testing H2, the GLMM comprised year and Julian day as fixed continuous effects and stationID and yearID as categorical random terms ($N = 1369$). Finally, we tested the relationships between the changes in mean cell size and environmental variables (H4) with a GLMM comprising fixed effects of temperature, pH, salinity as well as log transformed concentrations of TN, TP, Si, and SPM. Log-transformation was conducted to conform the data to normality. In this model, stationID and yearID appeared as categorical random terms. As environmental information was not available for all stations, the number of samples in this analysis was reduced to $N = 525$.

Sensitivity analyses

We conducted a series of sensitivity analyses to make sure that our results do not depend on model specification or analysis decisions. First, we reran the models testing H1, H3, and H4 for the entire data set, that is, including the taxa that were not identified to species level. This increases the number of measurements for H1 to 344,578 (all measurements) and 54,886 (species-specific mean size per sample), for H3 to 1705 samples and H4 to 646 samples (as more samples met the cut-off criterion of 10 observations for calculating mean cell size). An analogous sensitivity analysis for H2 was not useful, as to assure that the species-specific trends reflect the same, clearly identified species, only fully identified taxa were used.

Second, the use of yearID as additional random effect has proven useful in other contexts (Gülzow et al. 2019; Werner et al. 2020), but is still under discussion (Seibold et al. 2021). Therefore, we redid the model for H1 without yearID. Third, the first year of observation in a newly established monitoring may differ as approaches need to be streamlined. Therefore, we checked whether results depended on the first year of the time series (2006) and used the model for H1 with data from 2007 onwards. For H2, we finally tested whether using ordinary least square regressions resulted in different outcomes than the GLMM-derived slopes.

Results

Cell size of the Wadden Sea phytoplankton varied several orders of magnitude across all samples (Fig. 1A) and at any point in time (Fig. 1B). Distinct peaks of highly frequent cell

Table 1. Mixed effect linear model on species-specific cell size over time based on all available measurements and species-specific means per sample, respectively. The table gives the estimate and its CI as well as significance level for the intercept and the fixed effects of year and Julian day (see Methods). For the random terms, we show the variance represented by the random factors (τ_{00}), the intraclass correlation coefficient (ICC) for mixed models (i.e., the proportion of variance explained by the grouping structure), the number of unique levels in the random factors (N), the number of observations total (Obs.), and the marginal (mR^2) as well as conditional (cR^2) explained variance.

Predictors	All measurements			Sample means		
	Estimates	CI	p	Estimates	CI	p
Intercept	89.046	69.612–108.479	< 0.001	85.234	62.631–107.823	< 0.001
Year	−0.041	−0.050 to −0.031	< 0.001	−0.039	−0.050 to −0.027	< 0.001
Julian day	−0.001	−0.001 to −0.001	< 0.001	−0.001	−0.001 to −0.001	< 0.001
<i>Random effects</i>						
σ^2	0.37			0.41		
τ_{00}	2.78 _{species:(genus:(order:[class:phylum]))}			2.67 _{species:(genus:(order:[class:phylum]))}		
	2.33 _{genus:(order:[class:phylum])}			2.15 _{genus:(order:[class:phylum])}		
	1.23 _{order:(class: phylum)}			1.40 _{order:(class: phylum)}		
	1.04 _{class: phylum}			1.01 _{class:phylum}		
	1.47 _{phylum}			1.50 _{phylum}		
	0.00 _{stationID}			0.00 _{stationID}		
ICC	0.01 _{yearID}			0.01 _{yearID}		
	0.96			0.96		
N	162 _{species}			162 _{species}		
	85 _{genus}			85 _{genus}		
	40 _{order}			40 _{order}		
	12 _{class}			12 _{class}		
	8 _{phylum}			8 _{phylum}		
	14 _{yearID}			14 _{yearID}		
Obs.	20 _{stationID}			20 _{stationID}		
	273,881			29,678		
mR^2/cR^2	0.003/0.960			0.003/0.956		

sizes emerged throughout the size spectrum and these remained virtually unchanged between the full data and the reduced set with only taxa identified to species level (Fig. 1A). The median percentage of total sample biomass recovered in the species-level data was 89.9%.

The overall model on all measured cells found a major proportion of the variance associated to the random intercepts in the nested phylogeny (phylum, class, order, genus, species), whereas location (stationID) and timing (yearID) did not contribute substantially to the conditional R^2 (Table 1). Portions of the variance were associated to all taxonomic levels from species to phylum, indicating that size is phylogenetically constrained on morphology and physiology.

On top of these random intercepts, both fixed effects, year and Julian Day, were significant negative predictors of cell size (Table 1; Fig. 1B), indicating that cell sizes decreased over the duration of the monitoring time series and toward summer. These reductions in size remained consistent and nearly identical when redoing the analyses on sample mean cell size per species rather than all measured cells (Table 1). The slopes of

the temporal decline per year (−0.041 and −0.039 for all measured cells and species means per sample, respectively) are for log-transformed cell size and reflect a decline in average size by ~ 33% over a decade, thus a cell of 1000 μm^3 would be reduced to (or replaced by) a cell of 670 μm^3 in 10 yr.

Sensitivity analyses showed that these outcomes are not strongly dependent on model choices, as neither the model without yearID as a random factor nor the model without the first year 2006 showed different results (Supporting Information Table S1). Redoing the model for all taxa, also for those not identified to species, did not alter the overall results either, irrespective whether using all measured cells or species-specific sample means (Supporting Information Table S1).

Testing for intraspecific trends, 63 of 73 species showed a decline in cell size over time (Fig. 2A,B), which in the GLMM was significant for 27 species (at $p < 0.1$) and for 55 species in the ordinary least square regressions (Supporting Information Table S2). Only three species showed significant increases in cell size according to the GLMMs. Consequently, the grand mean slope was significantly negative (random effect meta-

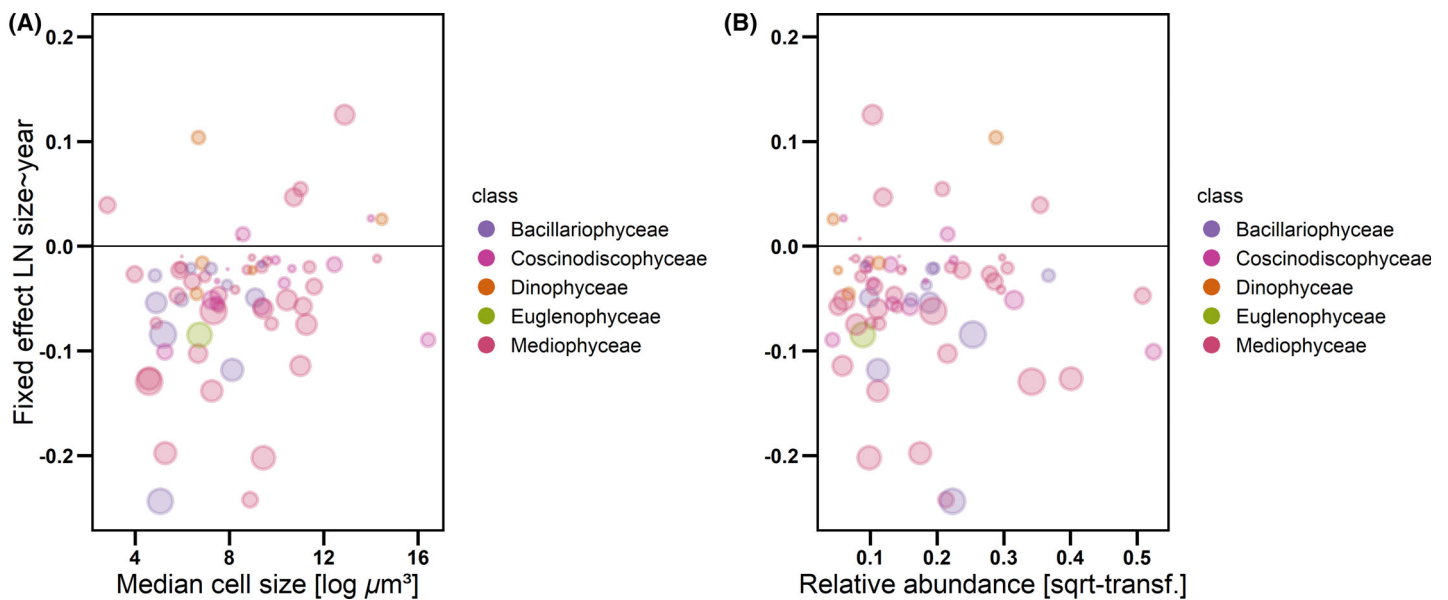


Fig. 2. Slopes from species-specific mixed effect linear models of natural log transformed cell size over year, plotted against the median cell size of the species (A) and their average relative abundance when present (B). Negative values indicate decreasing cell size, positive values increasing cell size with time. Symbol color is by class, symbol size is related to the ratio of slope to its standard error (larger symbols = more significant slopes). Correlations between slopes and cell size or relative abundance were not significant (Pearson’s $|r| < 0.12$, $p > 0.3$).

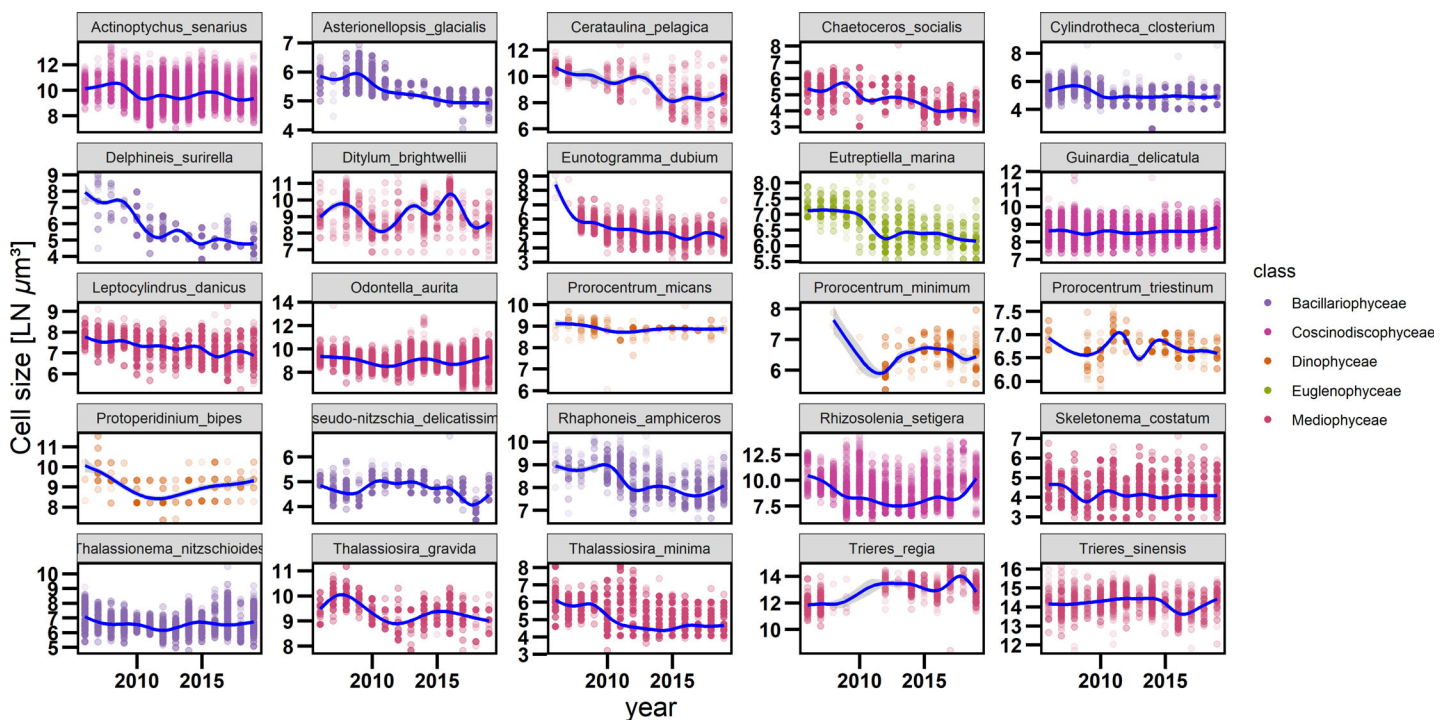


Fig. 3. Temporal change in the cell size of some dominant species in the monitoring time series of Wadden Sea phytoplankton, by color coded taxonomic class. Intensity increases with number of measurements. The 25 species represent a subset of the species listed in Table Supporting Information Table S2.

analysis, mean fixed effect of year = -0.045 , 95% confidence interval [CI] -0.060 to -0.030 , $p < 0.001$). Results were highly similar when ordinary least square slopes were used (Supporting

Information Table S2, mean slope = -0.056 , 95% CI -0.078 to -0.034 , $p < 0.001$). There was no obvious relationship change between the species’ slopes of size with time and either its average

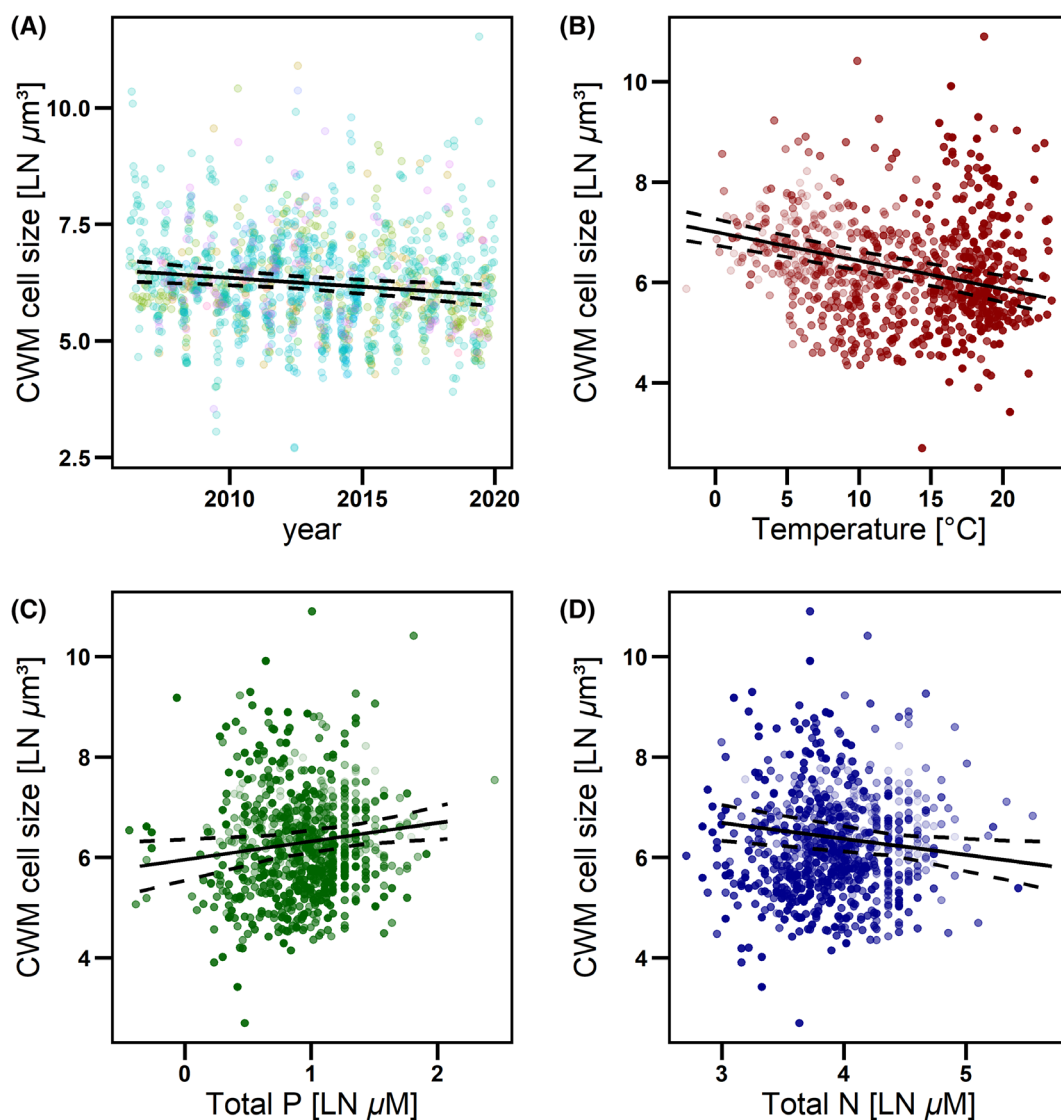


Fig. 4. (A) Community weighted mean cell size for 1710 samples in the Wadden Sea monitoring program over time. Black line is the significant fixed effect of time (year), dotted lines the 95% confidence interval of the predicted effect. (B–D) Raw data and predicted fixed effect of temperature (B), total P (C), and total N (D). In these panels shading reflects the transformed Julian Day variable, with denser shading for summer values.

size (Fig. 2A) or its average relative abundance (Fig. 2B), but from the 27 species experiencing significant size reductions, 25 were diatoms.

In Fig. 3, examples for such strong declines can be seen in *Asterionellopsis glacialis*, *Cerataulina pelagica*, *Chaetoceros socialis*, *Delphineis surirella*, *Eunotogramma dubium*, *Rhaphoneis amphiceros*, and *Thalassiosira minima*. The euglenophyte *Eutreptiella marina* was a non-diatom species experiencing a similarly strong size reduction. Some of the most abundant diatoms also showed conspicuous declines, even though less steep, such as *Actinoptychus senarius*, *Cylindrotheca closterium*, or *Leptocylindrus danicus*. However, some species counteracted this overall trend, as they showed an increase in size over time, which was true for the diatom *Trieres regia*. Other, highly

abundant species, such as *Pseudo-nitzschia delicatissima*, *Skeletonema costatum*, *Guinardia delicatula*, *Thalassionema nitzschioides*, or *Odontella aurita* showed weak to absent changes in size with time. Dinoflagellates (*Prorocentrum micans*, *Prorocentrum triestinum*, *Protoperidinium bipes*) generally seemed to be less responsive. Some species, here exemplified by the diatoms *Ditylum brightwelli* and *Thalassiosira gravida*, underwent more cyclic changes in size.

When characterizing the size of the entire community by weighted mean cell sizes, we again observed a significant decline over the years as well as toward summer within years (Fig. 4A; Table 2). The strong cyclic pattern of seasonal reductions overlays an interannual trend (Table 2, slope = -0.035), which corresponds in magnitude to the slopes reported above.

Table 2. Community weighted mean cell sizes in Wadden Sea phytoplankton analyzed in relation to temporal and environmental factors in a GLMM. Mean cell size is based on taxa identified to species level, see Supporting Information Table S3 for an alternative with all taxa. Year and transformed Julian day (see Methods section) were fixed effects in the temporal model. In the two environmental models, variables included were measured alongside the phytoplankton samples and included temperature (°C), TN (all nutrients in $\mu\text{mol L}^{-1}$), TP, Si, pH, salinity and SPM. [log] denotes natural-log transformed variables. The annual environmental model comprises annual means, which reduces the number of observations to 43, therefore a reduced set of predictors was used. The estimate, its confidence interval and the significance level is noted for each fixed effect. The random effects are reported as in Table 1. The environmental model is done on a subset of the temporal data, as abiotic variables were only monitored for four stations. Significance levels $p < 0.05$ are highlighted in bold.

Pred	Temporal model		Environmental model		Annual Env model	
	Est/CI	<i>p</i>	Est/CI	<i>p</i>	Est/CI	<i>p</i>
Int	83.050	0.003	6.188	0.001	11.640	<0.001
	27.412–138.687		2.400–9.977		8.618–14.662	
Year	–0.038	0.007				
	–0.066 to –0.010					
Julian day	–0.004	<0.001				
	–0.005 to –0.003					
Temp			–0.057	<0.001	–0.051	0.147
			–0.075 to –0.039		–0.120 to 0.018	
TN [log]			–0.319	0.022	–1.349	0.003
			–0.592 to –0.046		–2.252 to –0.445	
TP [log]			0.368	0.019	0.737	0.183
			0.061–0.674		–0.348 to 1.822	
SPM [log]			–0.010	0.872		
			–0.136 to 0.115			
Si [log]			–0.092	0.177		
			–0.227 to 0.042			
pH			0.269	0.238		
			–0.178 to 0.716			
Salinity			–0.017	0.152		
			–0.040 to 0.006			
<i>Random effects</i>						
σ^2	0.99		0.72		0.19	
τ_{00}	0.01 _{stationID}		0.01 _{stationID}		0.04 _{stationID}	
	0.03 _{yearID}		0.04 _{yearID}			
ICC	0.04		0.07		0.16	
<i>N</i>	19 _{stationID}		4 _{stationID}		4 _{stationID}	
	14 _{yearID}		12 _{yearID}			
Obs.	1369		525		43	
mR^2/cR^2	0.051/0.087		0.083/0.147		0.254/0.373	

When testing the impact of environmental factors, the conditional R^2 increased to 14.7% (Table 2), and temperature and nutrients turned out to be the most important predictors (Fig. 4B–D). Smaller mean cell size was strongly associated to high temperatures and marginally significant to low TP and high TN (Table 2). Because seasonal variation in temperature and nutrients was larger than the interannual trend (Supporting Information Fig. S2), we used annual averages of mean cell size, temperature, TN and TP in a separate model to test whether the observed results were solely inferred by seasonality. We qualitatively found again that mean cell size

declined with temperature and TN but increased with TP (Table 2). However, the temperature trend turned nonsignificant, whereas the TN effects appeared even stronger than in the previous model.

Redoing the model for mean cell size based on all taxa (i.e., also those not identified to species level) did result in slight changes in the outcome (Supporting Information Table S3). In the temporal model, the interannual decrease in mean cell size became marginally nonsignificant ($p = 0.07$), whereas the seasonal decline towards summer remained unchanged. In the environmental model, the decline in mean

cell size with temperature pertained to the full data set as well, but nutrients were not significant in that model. Instead, small cell size was associated to low suspended particulate matter concentrations and high pH as well as salinity.

Discussion

Using a long-term monitoring data set from the Lower Saxony section of the Wadden Sea, we showed significant reductions in phytoplankton cell size over the observation period of 14 yr (hypothesis H1). This interannual decline in cell size was observed in 63 out of 73 species in this data set (H2), 25 of the 27 significant declines were associated to diatoms. Even though three species showed opposing trends and others no temporal trends, the average intraspecific slope was significantly smaller than zero. The same pattern could be observed at the community level, where mean cell size declined over time and toward summer (H3). Lower mean cell size was consistently associated to high temperatures (H4), whereas the impact of nutrients and other environmental factors differed when analyzing all taxa or the subset identified to species level only.

We tested the sensitivity of our results to details of the model setup and found our main results to be unaffected. The decline of cell size was consistent irrespective of whether we looked at all taxa or only those identified to species level, included or excluded the first year or yearID as additional random term. The only difference we observed was for the nutrient effects on mean cell size as observed in our environmental model (cf. Table 2 and Supporting Information Table S3), which disappeared when we extended the model to all samples (also those that had less than 10 species identified to species level).

Our analyses suggest that the observed overall decline in cell size occurs both for individuals within species as for the composition of the community. Whereas the range of size changes in species is large (Fig. 2), the average intraspecific slope (-0.056) and the slope of the decline in mean cell size (-0.038) are highly comparable. Moreover, the decline not only appeared across years but also toward summer within years. The generality of the decline in cell size at different time scales and both at the community and species level indicates that the reason behind the decline might be rather deeply rooted in general metabolic principles such as the effects of temperature (Brown et al. 2004) or resource requirements (Irwin et al. 2006). However, the quest for disentangling drivers for changing size structure in these long-term monitoring data is challenged by covariances between temperature and nutrient concentrations. Moreover, other temporal analyses corresponding to ours are largely missing such that we mainly have to relate to information from spatial patterns of marine phytoplankton or experiments to explain the impact of the environmental factors on cell size. Still, nutrients declined and temperature increased both toward summer and

over the entire time period (Supporting Information Fig. S2), which make them potential key drivers for the observed reduction in cell size at both time scales.

Declines in the size of unicellular species with temperature have been predicted and observed (Atkinson et al. 2003; Forster et al. 2012; Bernhard et al. 2018). Declines in cell size have also been observed in climate warming experiments (Daufresne et al. 2009; Yvon-Durocher et al. 2011). We see seasonal variation of sea surface temperatures of $> 15^{\circ}\text{C}$ and an interannual increase by 2.1°C over the 14 yr of measurement (Supporting Information Fig. S2A), which is consistent with the significant upwards trends in surface temperature found in the region since 1980s (van Aken 2010; Desmit et al. 2020). However, the magnitude of change in cell size we observe is much higher than predicted. For instance, Atkinson et al. (2003) found a 2.5% decline per $^{\circ}\text{C}$ for protists, which would translate into an expected 5% decrease in the Wadden Sea phytoplankton cell size, whereas we see a decline of 30%. Thus, while temperature remains a candidate factor, its effects potentially are multiplied by other factors such as declining nutrient concentrations (van Beusekom et al. 2019) or changes in size-selective grazing.

At macroecological scales, low nutrient concentrations are often coupled with high SST (Acevedo-Trejos et al. 2013; Mousing et al. 2014), as both are primarily driven by thermal stratification (Sarmiento et al. 2004). The water column stratification induced by increasing temperature enhances the effect of cell sinking on the biomass loss (Ryabov and Blasius 2008) and because sinking rates increase with cell size (Portalier et al. 2016; Durante et al. 2019), the stratification gives an additional advantage to small cells in competition with larger cells. The Lower Saxony Wadden Sea under consideration in the current study (Supporting Information Fig. S1), however, is a shallow, tidally energetic system, characterized by strong horizontal salinity gradients. It is also subject to intermittent stratification driven by tidal straining (Burchard et al. 2008), depending also on the wind direction, phase of the spring-neap cycle and riverine discharge events (Chegini et al. 2020). In this highly dynamic area, such short-lived stratification events are not likely to have systematic effects on the nutrient environment of phytoplankton.

More directly though, a reduction in nutrients driven by riverine loadings from Ems and Weser, which in turn is a result of measures taken to reduce eutrophication of the North Sea (van Beusekom 2019), may be relevant, locally reflected by reduced TN and TP in recent years at the Wadden Sea stations we inspected (Supporting Information Fig. S2). We found smaller mean cell size to be associated to low TP periods of time, and thus potential P-limitation. Given a high N : P ratio (mean molar ratio of TN : TP across the stations = 22.2 ± 9.1), N is likely not limiting for a majority of the year (Loebl et al. 2009), except by the end of summer when P is released from sediments and N is removed by benthic denitrification (van Beusekom et al. 2019). This corresponds to the macroecological finding that smaller phytoplankton cells are

considered to dominate over larger cells under low nutrient supply regimes, for instance in the low-latitude oligotrophic gyres of the ocean, as detected by synoptic in situ observations (Marañón et al. 2012; Marañón 2015; Mousing et al. 2018) and by remote sensing products (Kostadinov et al. 2010). This pattern is often explained by higher nutrient affinity of smaller cells (Kiørboe 1993; Irwin et al. 2006; Litchman et al. 2007), assuming that low nutrients select for small cells (Ward et al. 2012; Marañón et al. 2015; Acevedo-Trejos et al. 2018). At the same time, low nutrients may also be the consequence of a dominance of small cells, as decreased nutrient concentrations may be induced by increased consumption of nutrients by small cells attributable to their high nutrient affinity (Edwards et al. 2012) and lower resource requirements. It should be noted though that the TP concentrations in the Wadden Sea remains high compared to oligotrophic open ocean waters. In addition, the TP effect in the GLMMs was not as consistent as the temperature effect and amended by an apparent negative relationship between cell size and the potentially not limiting nitrogen concentrations. Thus, while the changing nutrient concentrations likely contribute to the observed size changes, we are not able to fully quantify this relationship and its interaction with the temperature effect.

A third potential driver of altered cell size structure is grazing, but we have no direct observation on the intensity of feeding by zooplankton and filtering macroinvertebrates in the Wadden Sea area, let alone an estimate of how much the size structure is affected by consumers. However, typical ranges of preferred food for copepods (Sommer and Sommer 2006) or mussels (Strohmeier et al. 2012) are rather at the medium to large range of species, whereas escape from predation can be considered the major advantage of the largest cells (Kiørboe 1993; Irigoien et al. 2005; Cloern 2018). Therefore, potential shifts in grazing pressure during the observation period are well able to contribute to the observed shifts in cell size. However, the extent of this top-down effect on phytoplankton size remains speculative at this point.

At the same time, it is to be expected that the observed reduction in cell size by itself will trigger changes in the consumer community. In experiments, warming induced reductions in phytoplankton cell size reduced the grazing efficiency of the metazoan zooplankton, but increased the role of protistan grazers such as ciliates (Aberle et al. 2012). A stronger link between phytozooplankton and protozooplankton will potentially result in altered matter and energy flow in pelagic systems (Sommer et al. 2012; Aberle et al. 2015). Thus, considering shifts in cell size structure is a core ingredient in predictions of responses of marine and freshwater systems to changing environmental conditions (Klauschies et al. 2012).

Another consequence of altered size structure we expect is changes in biodiversity and morphological composition of phytoplankton, as the size of unicellular algae is closely related to the diversity of species and cell shapes (Ryabov et al. 2021). Cells of intermediate volume (1000 to

10,000 μm^3) comprise the greatest species and morphological diversity, including a full range from flat to externally elongated cell shapes. In contrast, smaller and larger classes are less species-rich and comprise predominantly compact cell shapes, such as spheres or cubes. Thus, a shift of the cell-size distribution towards small cells may result in a corresponding change of the pool of viable species and cell shapes and may indirectly alter the diversity of cell shapes and species.

Finally, our analysis makes a strong case for the time-consuming but more accurate measurement of cell volume per sample, with multiple individuals per species (Hillebrand et al. 1999). Many monitoring series use standard (literature or once measured) values per species, which not only precludes observing the intraspecific shifts in cell size we found here: Cell volumes are used to transfer abundances into carbon estimates (Montagnes et al. 1994; Menden-Deuer and Lessard 2000), which then are fed into carbon budgets. Moreover, carbon fixation per cell allometrically scales to cell size, whereas C-specific carbon fixation shows a nonlinear pattern (Taguchi 1976; Marañón et al. 2007; Malerba et al. 2021). Not accounting for temporal shifts in cell size might thus lead to highly biased estimates for phytoplankton biomass and performance.

Data availability statement

The data used for this analyses and the complete code are available at Zenodo (DOI: <https://doi.org/10.5281/zenodo.5799263>, URL: <https://zenodo.org/record/5799263>).

References

- Aberle, N., B. Bauer, A. Lewandowska, U. Gaedke, and U. Sommer. 2012. Warming induces shifts in microzooplankton phenology and reduces time-lags between phytoplankton and protozoan production. *Mar. Biol.* **159**: 2441–2453. doi:[10.1007/s00227-012-1947-0](https://doi.org/10.1007/s00227-012-1947-0)
- Aberle, N., A. M. Malzahn, A. M. Lewandowska, and U. Sommer. 2015. Some like it hot: The protozooplankton-copepod link in a warming ocean. *Mar. Ecol. Prog. Ser.* **519**: 103–113. doi:[10.3354/meps11081](https://doi.org/10.3354/meps11081)
- Acevedo-Trejos, E., G. Brandt, A. Merico, and S. L. Smith. 2013. Biogeographical patterns of phytoplankton community size structure in the oceans. *Glob. Ecol. Biogeogr.* **22**: 1060–1070. doi:[10.1111/geb.12071](https://doi.org/10.1111/geb.12071)
- Acevedo-Trejos, E., E. Marañón, and A. Merico. 2018. Phytoplankton size diversity and ecosystem function relationships across oceanic regions. *Proc. Roy. Soc. B Biol. Sci.* **285**: 2180621. doi:[10.1098/rspb.2018.0621](https://doi.org/10.1098/rspb.2018.0621)
- Atkinson, D., B. J. Ciotti, and D. J. S. Montagnes. 2003. Protists decrease in size linearly with temperature: Ca. 2.5% degrees C⁻¹. *Proc. R. Soc. Lond. Ser. B Biol. Sci.* **270**: 2605–2611. doi:[10.1098/rspb.2003.2538](https://doi.org/10.1098/rspb.2003.2538)

- Bates, D., M. Mächler, B. Bolker, and S. Walker. 2015. Fitting linear mixed-effects models using lme4. *J. Stat. Softw.* **67**: 48.
- Bernhard, J. R., J. M. Sunday, and M. I. O'Connor. 2018. Metabolic theory and the temperature-size rule explain the temperature dependence of population carrying capacity. *Am. Nat.* **192**: 687–697. doi:10.1086/700114
- Branco, P., M. Egas, S. R. Hall, and J. Huisman. 2020. Why do phytoplankton evolve large size in response to grazing? *Am. Nat.* **195**: E20–E37. doi:10.1086/706251
- Brown, J. H., J. F. Gillooly, A. P. Allen, V. M. Savage, and G. B. West. 2004. Toward a metabolic theory of ecology. *Ecology* **85**: 1771–1789. doi:10.1890/03-9000
- Bruelheide, H., and others. 2018. Global trait–environment relationships of plant communities. *Nat. Ecol. Evol.* **2**: 1906–1917. doi:10.1038/s41559-018-0699-8
- Burchard, H., G. Flöser, J. V. Staneva, T. H. Badewien, and R. Riethmüller. 2008. Impact of density gradients on net sediment transport into the Wadden Sea. *J. Phys. Oceanogr.* **38**: 566–587. doi:10.1175/2007JPO3796.1
- Chegini, F., and others. 2020. Processes of stratification and destratification during an extreme river discharge event in the German Bight ROFI. *J. Geophys. Res. Oceans* **125**: e2019JC015987.
- Cloern, J. E. 2018. Why large cells dominate estuarine phytoplankton. *Limnol. Oceanogr.* **63**: S392–S409. doi:10.1002/lno.10749
- Craine, J. M., W. G. Lee, W. J. Bond, R. J. Williams, and L. C. Johnson. 2005. Environmental constraints on a global relationship among leaf and root traits of grasses. *Ecology* **86**: 12–19. doi:10.1890/04-1075
- Daskalova, G. N., A. B. Phillimore, and I. H. Myers-Smith. 2021. Accounting for year effects and sampling error in temporal analyses of invertebrate population and biodiversity change: A comment on Seibold and others. 2019. *Insect Conserv. Divers.* **14**: 149–154. doi:10.1111/icad.12468
- Daufresne, M., K. Lengfellner, and U. Sommer. 2009. Global warming benefits the small in aquatic ecosystems. *Proc. Natl. Acad. Sci. USA* **106**: 12788–12793.
- Desmit, X., and others. 2020. Changes in chlorophyll concentration and phenology in the North Sea in relation to deoxygenation and sea surface warming. *Limnol. Oceanogr.* **65**: 828–847. doi:10.1002/lno.11351
- DuRand, M. D., R. J. Olson, and S. W. Chisholm. 2001. Phytoplankton population dynamics at the Bermuda Atlantic time-series station in the Sargasso Sea. *Deep-Sea Res. II Top. Stud. Oceanogr.* **48**: 1983–2003. doi:10.1016/S0967-0645(00)00166-1
- Durante, G., A. Basset, E. Stanca, and L. Roselli. 2019. Allometric scaling and morphological variation in sinking rate of phytoplankton. *J. Phycol.* **55**: 1386–1393. doi:10.1111/jpy.12916
- Edwards, K. F., M. K. Thomas, C. A. Klausmeier, and E. Litchman. 2012. Allometric scaling and taxonomic variation in nutrient utilization traits and maximum growth rate of phytoplankton. *Limnol. Oceanogr.* **57**: 554–566. doi:10.4319/lno.2012.57.2.0554
- Edwards, K. F., M. K. Thomas, C. A. Klausmeier, and E. Litchman. 2015. Light and growth in marine phytoplankton: Allometric, taxonomic, and environmental variation. *Limnol. Oceanogr.* **60**: 540–552. doi:10.1002/lno.10033
- Finkel, Z. V., J. Beardall, K. J. Flynn, A. Quigg, T. A. V. Rees, and J. A. Raven. 2010. Phytoplankton in a changing world: Cell size and elemental stoichiometry. *J. Plankton Res.* **32**: 119–137.
- Follows, M. J., and Dutkiewicz, S. 2011. Modeling diverse communities of marine microbes. *Annual Review of Marine Science* **3**: 427–451. doi:10.1146/annurev-marine-120709-142848
- Forster, J., A. G. Hirst, and D. Atkinson. 2012. Warming-induced reductions in body size are greater in aquatic than terrestrial species. *Proc. Natl. Acad. Sci. USA* **109**: 19310–19314.
- Grasshoff, K., M. Ehrhardt, and K. Kremling. 1983. *Methods of seawater analysis*, 2nd ed. Verlag Chemie.
- Grover, J. P. 1991. Resource competition in a variable environment: Phytoplankton growing according to the variable-internal-stores model. *Am. Nat.* **138**: 811–835. doi:10.1086/285254
- Guiry M.D. & Guiry G.M. (2021). *AlgaeBase*. Available from <https://www.algaebase.org>, DOI: 10.1126/sciadv.abh2525
- Gülzow, N., Y. Wahlen, and H. Hillebrand. 2019. Metecosystem dynamics of marine phytoplankton alters resource use efficiency along stoichiometric gradients. *Am. Nat.* **193**: 35–50. doi:10.1086/700835
- Hanslik, M., J. Rahmel, M. Bätje, S. Knieriemen, G. Schneider, and S. Dick. 1998. *Der Jahresgang blütenbildender und toxischer Algen an der niedersächsischen Küste seit 1982*. Umweltbundesamt Texte Bonn.
- Hillebrand, H., C. D. Duerksen, D. B. Kirschtel, U. Pollinger, and T. Zohary. 1999. Biovolume calculation for pelagic and benthic microalgae. *J. Phycol.* **35**: 403–424.
- Hillebrand, H., E. Acevedo-Trejos, S. D. Moorthi, A. Ryabov, M. Striebel, P. Thomas, and M. L. Schneider. 2021. Cell size as driver and sentinel of phytoplankton community structure and functioning. *Funct. Ecol.* doi:10.1111/1365-2435.13986
- Huete-Ortega, M., E. Marañón, M. Varela, and A. Bode. 2010. General patterns in the size scaling of phytoplankton abundance in coastal waters during a 10-year time series. *J. Plankton Res.* **32**: 1–14.
- Irigoiien, X., K. J. Flynn, and R. P. Harris. 2005. Phytoplankton blooms: A “loophole” in microzooplankton grazing impact? *J. Plankton Res.* **27**: 313–321. doi:10.1093/plankt/fbi011
- Irwin, A. J., Z. V. Finkel, O. M. E. Schofield, and P. G. Falkowski. 2006. Scaling-up from nutrient physiology to

- the size-structure of phytoplankton communities. *J. Plankton Res.* **28**: 459–471. doi:[10.1093/plankt/fbi148](https://doi.org/10.1093/plankt/fbi148)
- Kattge, J., and others. 2011. TRY—A global database of plant traits. *Glob. Chang. Biol.* **17**: 2905–2935. doi:[10.1111/j.1365-2486.2011.02451.x](https://doi.org/10.1111/j.1365-2486.2011.02451.x)
- Kerimoglu, O., D. Straile, and F. Peeters. 2012. Role of phytoplankton cell size on the competition for nutrients and light in incompletely mixed systems. *J. Theor. Biol.* **300**: 330–343. doi:[10.1016/j.jtbi.2012.01.044](https://doi.org/10.1016/j.jtbi.2012.01.044)
- Kjørboe, T. 1993. Turbulence, phytoplankton cell size, and the structure of pelagic food webs, p. 1–72. *In* B. JHS and A. J. Southward [eds.], *Advances in marine biology*. Academic Press.
- Klauschies, T., B. Bauer, N. Aberle-Malzahn, U. Sommer, and U. Gaedke. 2012. Climate change effects on phytoplankton depend on cell size and food web structure. *Mar. Biol.* **159**: 2455–2478. doi:[10.1007/s00227-012-1904-y](https://doi.org/10.1007/s00227-012-1904-y)
- Kleyer, M., and others. 2008. The LEDA Traitbase: A database of life-history traits of the Northwest European flora. *J. Ecol.* **96**: 1266–1274. doi:[10.1111/j.1365-2745.2008.01430.x](https://doi.org/10.1111/j.1365-2745.2008.01430.x)
- Kostadinov, T. S., D. A. Siegel, and S. Maritorena. 2010. Global variability of phytoplankton functional types from space: Assessment via the particle size distribution. *Biogeosciences* **7**: 3239–3257. doi:[10.5194/bg-7-3239-2010](https://doi.org/10.5194/bg-7-3239-2010)
- Larsson, U., and A. Hagström. 1982. Fractionated phytoplankton primary production, exudate release and bacterial production in a Baltic eutrophication gradient. *Mar. Biol.* **67**: 57–70. doi:[10.1007/BF00397095](https://doi.org/10.1007/BF00397095)
- Lewandowska, A., and U. Sommer. 2010. Climate change and the spring bloom: A mesocosm study on the influence of light and temperature on phytoplankton and mesozooplankton. *Mar. Ecol. Prog. Ser.* **405**: 101–111. doi:[10.3354/meps08520](https://doi.org/10.3354/meps08520)
- Litchman, E., C. A. Klausmeier, O. M. Schofield, and P. G. Falkowski. 2007. The role of functional traits and trade-offs in structuring phytoplankton communities: Scaling from cellular to ecosystem level. *Ecol. Lett.* **10**: 1170–1181. doi:[10.1111/j.1461-0248.2007.01117.x](https://doi.org/10.1111/j.1461-0248.2007.01117.x)
- Litchman, E., and C. A. Klausmeier. 2008. Trait-based community ecology of phytoplankton. *Annu. Rev. Ecol. Evol. Syst.* **39**: 615–639. doi:[10.1146/annurev.ecolsys.39.110707.173549](https://doi.org/10.1146/annurev.ecolsys.39.110707.173549)
- Litchman, E., C. A. Klausmeier, and K. Yoshiyama. 2009. Contrasting size evolution in marine and freshwater diatoms. *Proc. Natl. Acad. Sci. U.S.A.* **106**: 2665–2670.
- Loebl, M., F. Colijn, J. E. E. van Beusekom, J. G. Baretta-Bekker, C. Lancelot, C. J. M. Philippart, V. Rousseau, and K. H. Wiltshire. 2009. Recent patterns in potential phytoplankton limitation along the Northwest European continental coast. *J. Sea Res.* **61**: 34–43. doi:[10.1016/j.seares.2008.10.002](https://doi.org/10.1016/j.seares.2008.10.002)
- Malerba, M. E., D. J. Marshall, M. M. Palacios, J. A. Raven, and J. Beardall. 2021. Cell size influences inorganic carbon acquisition in artificially selected phytoplankton. *New Phytol.* **229**: 2647–2659. doi:[10.1111/nph.17068](https://doi.org/10.1111/nph.17068)
- Marañón, E. 2015. Cell size as a key determinant of phytoplankton metabolism and community structure. *Ann. Rev. Mar. Sci.* **7**: 241–264. doi:[10.1146/annurev-marine-010814-015955](https://doi.org/10.1146/annurev-marine-010814-015955)
- Marañón, E., P. Cermeno, J. Rodriguez, M. V. Zubkov, and R. P. Harris. 2007. Scaling of phytoplankton photosynthesis and cell size in the ocean. *Limnol. Oceanogr.* **52**: 2190–2198. doi:[10.4319/lo.2007.52.5.2190](https://doi.org/10.4319/lo.2007.52.5.2190)
- Marañón, E., P. Cermeno, M. Latasa, and R. D. Tadonleke. 2012. Temperature, resources, and phytoplankton size structure in the ocean. *Limnol. Oceanogr.* **57**: 1266–1278. doi:[10.4319/lo.2012.57.5.1266](https://doi.org/10.4319/lo.2012.57.5.1266)
- Marañón, E., P. Cermeño, M. Latasa, and R. D. Tadonléké. 2015. Resource supply alone explains the variability of marine phytoplankton size structure. *Limnol. Oceanogr.* **60**: 1848–1854. doi:[10.1002/lno.10138](https://doi.org/10.1002/lno.10138)
- Margalef, R. 1978. Life-forms of phytoplankton as survival alternatives in an unstable environment. *Oceanol. Acta* **1**: 493–509.
- Menden-Deuer, S., and E. J. Lessard. 2000. Carbon to volume relationships for dinoflagellates, diatoms, and other protist plankton. *Limnol. Oceanogr.* **45**: 569–579. doi:[10.4319/lo.2000.45.3.0569](https://doi.org/10.4319/lo.2000.45.3.0569)
- Montagnes, D. J. S., J. A. Berges, P. J. Harrison, and F. J. R. Taylor. 1994. Estimating carbon, nitrogen, protein, and chlorophyll a from volume in marine phytoplankton. *Limnol. Oceanogr.* **39**: 1044–1060. doi:[10.4319/lo.1994.39.5.1044](https://doi.org/10.4319/lo.1994.39.5.1044)
- Moran, X. A. G., A. Lopez-Urrutia, A. Calvo-Diaz, and W. K. W. Li. 2010. Increasing importance of small phytoplankton in a warmer ocean. *Glob. Chang. Biol.* **16**: 1137–1144. doi:[10.1111/j.1365-2486.2009.01960.x](https://doi.org/10.1111/j.1365-2486.2009.01960.x)
- Mousing, E. A., M. Ellegaard, and K. Richardson. 2014. Global patterns in phytoplankton community size structure—evidence for a direct temperature effect. *Mar. Ecol. Prog. Ser.* **497**: 25.
- Mousing, E. A., K. Richardson, and M. Ellegaard. 2018. Global patterns in phytoplankton biomass and community size structure in relation to macronutrients in the open ocean. *Limnol. Oceanogr.* **63**: 1298–1312. doi:[10.1002/lno.10772](https://doi.org/10.1002/lno.10772)
- Mutshinda, C. M., Z. V. Finkel, C. E. Widdicombe, and A. J. Irwin. 2017. Phytoplankton traits from long-term oceanographic time-series. *Mar. Ecol. Prog. Ser.* **576**: 11–25. doi:[10.3354/meps12220](https://doi.org/10.3354/meps12220)
- NLWKN. 2013. Gewässerüberwachungssystem Niedersachsen, Gütemessnetz Übergangs- und Küstengewässer 2013. *Küstengewässer und Ästuar*: **6**: 50.
- Olenina, I., and others. 2006. Biovolumes and size-classes of phytoplankton in the Baltic Sea. *HELCOM Baltic Sea Environment Proceedings*: **106**: 144.
- Philippart, C. J. M., G. C. Cadée, W. van Raaphorst, and R. Riegman. 2000. Long-term phytoplankton-nutrient

- interactions in a shallow coastal sea: Algal community structure, nutrient budgets, and denitrification potential. *Limnol. Oceanogr.* **45**: 131–144. doi:[10.4319/lo.2000.45.1.0131](https://doi.org/10.4319/lo.2000.45.1.0131)
- Portalier, S. M. J., M. Cherif, L. Zhang, G. F. Fussmann, and M. Loreau. 2016. Size-related effects of physical factors on phytoplankton communities. *Ecol. Model.* **323**: 41–50. doi:[10.1016/j.ecolmodel.2015.12.003](https://doi.org/10.1016/j.ecolmodel.2015.12.003)
- Prins, T. C., X. Desmit, and J. G. Baretta-Bekker. 2012. Phytoplankton composition in Dutch coastal waters responds to changes in riverine nutrient loads. *J. Sea Res.* **73**: 49–62. doi:[10.1016/j.seares.2012.06.009](https://doi.org/10.1016/j.seares.2012.06.009)
- R Development Core Team. 2018. R: A language and environment for statistical computing (version 3.5.1). R Foundation for Statistical Computing.
- R Studio Team. 2018. RStudio: Integrated development for R (version 1.1.423). RStudio, Inc.
- Rasconi, S., A. Gall, K. Winter, and M. J. Kainz. 2015. Increasing water temperature triggers dominance of small freshwater plankton. *PLoS One* **10**: e0140449.
- Raunkiaer, C. 1907. Planteriget Livsformer og deres Betydning for Geografien. Gyldendalske Boghandel, Nordisk Forlag.
- Reynolds, C. S. 1984. Phytoplankton periodicity: The interactions of form, function and environmental variability. *Freshw. Biol.* **14**: 111–142. doi:[10.1111/j.1365-2427.1984.tb00027.x](https://doi.org/10.1111/j.1365-2427.1984.tb00027.x)
- Ryabov, A., O. Kerimoglu, E. Litchman, I. Olenina, L. Roselli, A. Basset, E. Stanca, and B. Blasius. 2021. Shape matters: The relationship between cell geometry and diversity in phytoplankton. *Ecol. Lett.* **24**: 847–861. doi:[10.1111/ele.13680](https://doi.org/10.1111/ele.13680)
- Ryabov, A. B., and B. Blasius. 2008. Population growth and persistence in a heterogeneous environment: The role of diffusion and advection. *Math. Model. Nat. Phenom.* **3**: 42–86. doi:[10.1051/mmnp:2008064](https://doi.org/10.1051/mmnp:2008064)
- Sarmiento, J. L., and others. 2004. Response of ocean ecosystems to climate warming. *Glob. Biogeochem. Cycles* **18**. GB3003. doi:[10.1029/2003GB002134](https://doi.org/10.1029/2003GB002134)
- Seibold, S., and others. 2021. Insights from regional and short-term biodiversity monitoring datasets are valuable: A reply to Daskalova et al. 2021. *Insect Conserv. Divers.* **14**: 144–148. doi:[10.1111/icad.12467](https://doi.org/10.1111/icad.12467)
- Sommer, U. 1988. Some size relationships in phytoflagellate motility. *Hydrobiologia* **161**: 125–131. doi:[10.1007/BF00044105](https://doi.org/10.1007/BF00044105)
- Sommer, U., and F. Sommer. 2006. Cladocerans versus copepods: The cause of contrasting top-down controls on freshwater and marine phytoplankton. *Oecologia* **147**: 183–194. doi:[10.1007/s00442-005-0320-0](https://doi.org/10.1007/s00442-005-0320-0)
- Sommer, U., and K. Lengfellner. 2008. Climate change and the timing, magnitude, and composition of the phytoplankton spring bloom. *Glob. Chang. Biol.* **14**: 1199–1208. doi:[10.1111/j.1365-2486.2008.01571.x](https://doi.org/10.1111/j.1365-2486.2008.01571.x)
- Sommer, U., N. Aberle, K. Lengfellner, and A. Lewandowska. 2012. The Baltic Sea spring phytoplankton bloom in a changing climate: An experimental approach. *Mar. Biol.* **159**: 2479–2490. doi:[10.1007/s00227-012-1897-6](https://doi.org/10.1007/s00227-012-1897-6)
- Strohmeier, T., Ø. Strand, M. Alunno-Bruscia, A. Duinker, and P. J. Cranford. 2012. Variability in particle retention efficiency by the mussel *Mytilus edulis*. *J. Exp. Mar. Biol. Ecol.* **412**: 96–102. doi:[10.1016/j.jembe.2011.11.006](https://doi.org/10.1016/j.jembe.2011.11.006)
- Suding, K. N., and others. 2008. Scaling environmental change through the community-level: A trait-based response-and-effect framework for plants. *Glob. Chang. Biol.* **14**: 1125–1140. doi:[10.1111/j.1365-2486.2008.01557.x](https://doi.org/10.1111/j.1365-2486.2008.01557.x)
- Taguchi, S. 1976. Relationship between photosynthesis and cell size of marine diatoms. *J. Phycol.* **12**: 185–189.
- Utermöhl, H. 1958. Zur Vervollkommnung der quantitativen Phytoplankton-Methodik. *Mitt. Int. Ver. Limnol.* **9**: 1–38.
- van Aken, H. M. 2010. Meteorological forcing of long-term temperature variations of the Dutch coastal waters. *J. Sea Res.* **63**: 143–151. doi:[10.1016/j.seares.2009.11.005](https://doi.org/10.1016/j.seares.2009.11.005)
- van Beusekom, J. E. E., and others. 2019. Wadden Sea eutrophication: Long-term trends and regional differences. *Front. Mar. Sci.* **6**: article 370 doi: [10.3389/fmars.2019.00370](https://doi.org/10.3389/fmars.2019.00370)
- Verity, P. G., and V. Smetacek. 1996. Organism life cycles, predation, and the structure of marine pelagic ecosystems. *Mar. Ecol. Prog. Ser.* **130**: 277–293. doi:[10.3354/meps130277](https://doi.org/10.3354/meps130277)
- Viechtbauer, W. 2010. Conducting meta-analyses in R with the metafor package. *J. Stat. Softw.* **36**: 1–48.
- Violle, C., M. L. Navas, D. Vile, E. Kazakou, C. Fortunel, I. Hummel, and E. Garnier. 2007. Let the concept of trait be functional! *Oikos* **116**: 882–892. doi:[10.1111/j.0030-1299.2007.15559.x](https://doi.org/10.1111/j.0030-1299.2007.15559.x)
- Ward, B. A., S. Dutkiewicz, O. Jahn, and M. J. Follows. 2012. A size-structured food-web model for the global ocean. *Limnol. Oceanogr.* **57**: 1877–1891. doi:[10.4319/lo.2012.57.6.1877](https://doi.org/10.4319/lo.2012.57.6.1877)
- Weigelt, P., C. König, and H. KrefT. 2020. GIFT—A Global Inventory of Floras and Traits for macroecology and biogeography. *J. Biogeogr.* **47**: 16–43.
- Werner, C. M., K. L. Stuble, A. M. Groves, and T. P. Young. 2020. Year effects: Interannual variation as a driver of community assembly dynamics. *Ecology* **101**: e03104. doi:[10.1002/ecy.3104](https://doi.org/10.1002/ecy.3104)
- Wiltshire, K. H., A. M. Malzahn, K. Wirtz, W. Greve, S. Janisch, P. Mangelsdorf, B. F. J. Manly, and M. Boersma. 2008. Resilience of North Sea phytoplankton spring bloom dynamics: An analysis of long-term data at Helgoland roads. *Limnol. Oceanogr.* **53**: 1294–1302. doi:[10.4319/lo.2008.53.4.1294](https://doi.org/10.4319/lo.2008.53.4.1294)
- Winder, M., J. E. Reuter, and S. G. Schladow. 2009. Lake warming favours small-sized planktonic diatom species.

Proc. Roy. Soc. B Biol. Sci. **276**: 427–435. doi:[10.1098/rspb.2008.1200](https://doi.org/10.1098/rspb.2008.1200)

Yvon-Durocher, G., J. M. Montoya, M. Trimmer, and G. Woodward. 2011. Warming alters the size spectrum and shifts the distribution of biomass in freshwater ecosystems. *Glob. Chang. Biol.* **17**: 1681–1694. doi:[10.1111/j.1365-2486.2010.02321.x](https://doi.org/10.1111/j.1365-2486.2010.02321.x)

Acknowledgments

We are grateful for all staff contributing to this data set by sampling, analyzing, and providing the data. We are especially indebted to Michael Hanslik, who curates the phytoplankton data at NLWKN. HH, LR, and JAC acknowledge funding by the INTERREG V A program Deutschland-Niederland of the European Union, project “Water quality” (201265); HH and LK further acknowledge funding by the German Science Foundation funded research unit DynaCom (DFG HI 848/26-1). OK acknowledges funding by the German Science Foundation (DFG KE 1970/2-1). AR was

partly supported by the Federal Ministry of Education and Research BMBF Germany Project PEKRIS II (03F0828), JCD by MARISCO (03F0836A). HIFMB is a collaboration between the Alfred-Wegener-Institute, Helmholtz-Center for Polar and Marine Research, and the Carl-von-Ossietzky University Oldenburg, initially funded by the Ministry for Science and Culture of Lower Saxony and the Volkswagen Foundation through the “Niedersächsisches Vorab” grant program (grant number ZN3285). Open Access funding enabled and organized by Projekt DEAL.

Conflict of Interest

The authors declare no conflict of interest.

Submitted 26 July 2021

Revised 22 November 2021

Accepted 12 December 2021

Associate editor: C. Elisa Schaum